Stickman: Towards a Human Scale Acrobatic Robot

Morgan T. Pope, Steven Christensen, David Christensen,
Anthony Simeonov, Grant Imahara, and Günter Niemeyer[1]

***Abstract*— Human performers have developed impressive acrobatic techniques over thousands of years of practicing the gymnastic arts. At the same time, robots have started to become more mobile and autonomous, and can begin to imitate these stunts in dramatic and informative ways. We present a simple two degree of freedom robot that uses a gravity-driven pendulum launch and produces a variety of somersaulting stunts. The robot uses an IMU and a laser range-finder to estimate its state mid-flight and actuates to change its motion both on and and off the pendulum. We discuss the dynamics of this behavior in a framework of acrobatic capability and present experimental results.**

I. Introduction

For thousands of years, people have been captivated by the aerial stunts of daring gymnasts and divers who swing, leap, twist, and flip through the air. Now that robots are becoming more mobile, intelligent, and aware, the ability to mimic these stunts presents several opportunities. Besides the interesting questions of robot design and control posed by this field, a robotic acrobat can help answer questions about how stunts are performed in ways that may be of use to elite gymnasts. In studies which investigate the physics of a given stunt, such as [1], some major difficulties in analysis exist. First, the inertia of the human can only be approximated, as disassembly for measuring each limb is infeasible. Second, a performer who attempts to make a specific change to their approach to a stunt might inadvertently change many variables at once. Thirdly, performer joint angles must be approximated from video, a difficulty compounded by the fact that many human joints do not have a fixed center of rotation relative to the limbs. A robotic performer is not inherently subject to these limitations, and so is an effective tool for exploring specific strategies of locomotion. Beyond this, an acrobatic robot pushes the limits of control, sensing, and fabrication in ways that could have relevance for robots in general.

In this paper, we present an acrobatic robot, Stickman as shown in Fig 1, that swings through the air on a pendulum, "tucks" to change its moment of inertia, releases, "untucks" to reduce its spin, and gracefully lands on its back on a foam mat as shown in Fig. 2 and in the multimedia attachment accompanying this paper. In discussing this effort, it is helpful to define a few basic metrics for measuring the capability and precision of an acrobatic robot and its accompanying launch system, as explained in Sec. III. After describing our robot and basic approach in more detail in

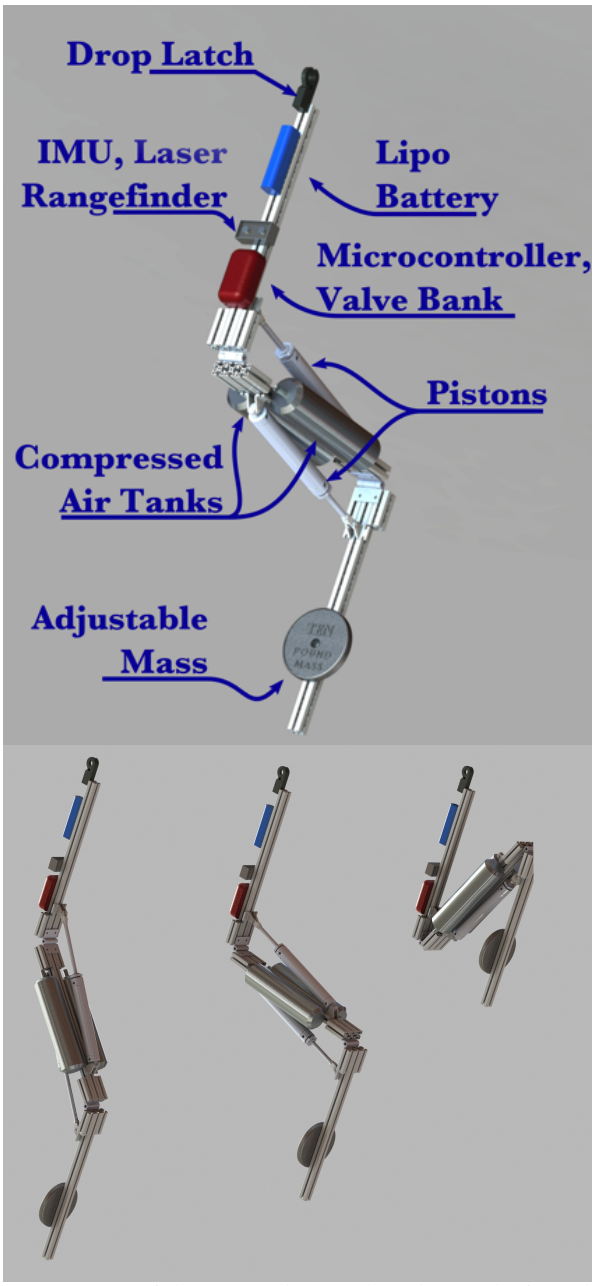

Fig. 1: Top: Stickman, a human-length acrobatic robot, consists of three links that can fold or unfold to tuck or untuck during a somersault. Bottom: Stickman folding into the tucked configuration.

[1]All authors affiliated with Disney Research, Glendale, CA 91201, USA. Email: {morgan.pope, gunter.niemeyer}@disneyresearch.edu

Sec. IV, we dive into the details of the system dynamics and our initial modeling efforts in Sec. V. Finally, in Sec. VI, we present results on the robot's performance of various stunts and the sensing and control efforts.

II. Background

In robotics, much work has been done on jumping [2]–[5] and hopping robots, of which [6] is a foundational example. Hopping and jumping robots are usually focused on total height rather than number of in-flight rotations, but they must nevertheless control their rotation in some way to achieve a stable landing and jump again. [7] uses a spinning rod to help ensure stability before executing a secondary jump off a vertical surface. The ParkourBot [8] uses gyroscopic stabilization to maintain heading as it performs multiple jumps in a simulated reduced-gravity environment. Other approaches use aerodynamic surfaces to control orientation, as in [9,10]. [11] uses an internal weight to orient correctly while on the ground before using rotors to take off for brief hopping flights.

Changing orientation during free fall has been explored recently by robots which use inertial tails to reorient themselves, a strategy also found in the natural world [12]. By actuating a tail with a relatively high moment of inertia, rapid changes in gross body orientation are possible [13], allowing robots to recover from unfavorable body orientations while falling [14]. Controls for a "cat robot" which used torque between two columnar halves to control final orientation were explored theoretically in [15], and a twisting robot was demonstrated in [16,17]. Inertia shaping for a humanoid robot has been explored through in [18]. All of these applications involve relatively low initial spin rates and perform less than a full revolution.

For somersaulting robots, [19] actively shapes angular momentum during the ground contact phase and have proposed a framework for control during a long airborne phase. Similarly, [20] characterizes angular momentum to inform control while in contact with the ground. Detailed simulations of higher-spin rate humanoid inertia shaping in [21,22] show the potential of this strategy for controlling free-fall landing conditions if it could be realized on a humanoid robot. The most relevant prior work of all is probably [23], in which a robot performed a somersault and moved its leg position to shape inertia in flight and land at a target angle. A similar control strategy is probably employed in the recent video of the Atlas robot ([24]) performing a backflip. There has also been work investigating the physics of swinging using a robot that could move along a ladder using alternating limbs [25].

This paper builds heavily off work to be presented at IROS 2017, in which a spinning brick-shaped robot used movable internal weights to change its inertia and fall through a narrow slot [26].

III. Quantifying Acrobatic Performance

In thinking of an acrobatic robot, it is helpful to define some basic metrics by which to measure the performance of a given design. Number of rotations about a given body axis seems a likely figure of merit, as this is the main way aerial stunts are categorized in diving and gymnastics. Peak height and total horizontal distance covered are also interesting measures of any ballistic leap, as they both give a sense of the scale of the motion. In this paper we will concentrate on horizontal distance because the indoor location of our test rig puts a practical limit on peak height.

In addition to the broad capabilities mentioned above, an acrobatic robot can also be judged by the precision with which it lands, both in terms of final location and final orientation.

These capabilities can be thought of as shared between the robot's launching apparatus and its ability to affect motion during flight. A jumping robot carries its launching apparatus on-board, and a flying or gliding robot uses aerodynamics to significantly change the trajectory of its center of mass during flight. Our approach uses a separate launching system and minimizes aerodynamic effects. This means that the final location is purely a function of the launch conditions, if we define the launch as being the point at which Stickman releases from the pendulum. The final orientation, and the amount of rotation preceding that final state, is a function both of the angular momentum and initial angle provided by the launch and the ability of the robot to change its angular velocity during flight. In gymnastics, the final orientation is an important measure of success; in robotics, landing in a predictable orientation can help protect the vulnerable components of the machine.

In the following, we demonstrate the capability to perform zero, one, and two flips; to throw the robot between 5 and 10 meters horizontally away from the pivot of the pendulum; to control landing location within a standard deviation of 0.3 meters; and to control landing orientation within a standard deviation of 30 degrees.

IV. Stickman and the Basic Approach

The robot, Stickman, consists of three aluminum links connected by hinges which allow it to transition from a collapsed "Z" configuration to an approximately straight line as shown in Fig 1. When untucked, Stickman is designed to be 7 feet tall to approximate the height of a human stunt performer with arms raised over his or her head. Air tanks store the energy used for actuation and a 12v Lithium Polymer battery pack powers the solenoid valves controlling the actuators. The basic construction of the prototype was influenced by a desire for easy reconfigurability, fast repair, and high peak actuator strength and power.

T-Slot aluminum extrusion was used to allow for reconfigurability of various components based on incremental findings. Both ends of the air pistons can be adjusted along the length of their links, allowing changes in torque profiles. A large extra weight can be added to the top or bottom link in order to adjust the robot's center of mass location and change in moment of inertia.

Pneumatic actuators were chosen for their high power density, and are actuated with solenoid valves that are

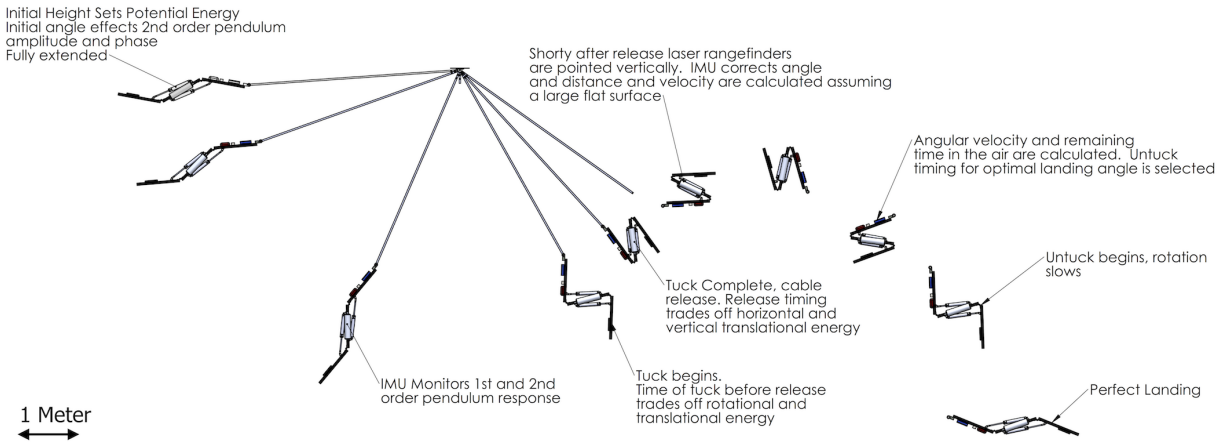

Fig. 2: Basic approach to performing a somersault stunt with Stickman. The robot is attached to a rigid pendulum and raised to the ceiling of the laboratory, approximately 6 meters above the ground. It releases from the ceiling, swings through an arc, begins to tuck and releases from the pendulum at a pre-determined time. It then attempts to estimate its height and velocity to calculate time in the air. When it predicts that untucking will result in the correct landing orientation, it commands an untuck and lands gently on its back on a foam mat.

triggered by the Arduino Micro controller board. The top link is outfitted with both a LIDAR-Lite v3 laser rangefinder and a 6-axis Invensense ICM 20602 inertial measurement unit which comprise the main inputs to the robot.

We use a gravity-driven pendulum to launch Stickman. By raising the robot nearly to the ceiling, we are able to inject significant energy into the launch. The long swing spreads out this acceleration over a large distance, making for relatively gentle accelerations. Stickman releases from the ceiling and the pendulum using two servo-driven quick release latches as illustrated in the accompanying multimedia attachment.

The joint attaching the robot to the pendulum will have a stiffness ranging from the theoretical extremes of zero (a pin-joint) to infinity (a rigid link). A rigid joint would turn the whole system into a simple compound pendulum with very predictable behavior, likely increasing the repeatability of landing position. However, this also constrains angular velocity to be a function of linear velocity, limiting the range of somersault ability. A pin joint creates a double pendulum, a chaotic system with high sensitivity to initial conditions. As a result, however, it is possible to decouple angular velocity from linear velocity and produce a larger range of launch conditions.

The basic sequence of Stickman performing a stunt is illustrated in Fig. 2. The logical flow of the robot's control scheme is illustrated in Fig. 3

An Optitrack motion capture system is used to provide reference position data.

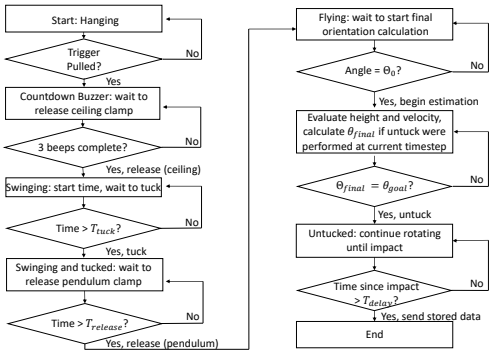

Fig. 3: Stickman control scheme logic diagram

V. Dynamics

A. Swinging Dynamics

The double pendulum is the classic example of a chaotic system, and becomes only more complicated when the possibility of tucking mid-swing is introduced. To evaluate this complexity and the range of capabilities of our system, we created a detailed model using Matlab's Simscape Multibody toolbox. The model consists of a two-link pendulum (a stiff torsional spring connects the top half of the pendulum to the bottom half to help approximate the first oscillatory mode of the beam), three rigid bodies for the robot, and two massless telescoping actuators to simulate the pistons, as diagrammed in Fig. 4.

As expected, the simulation is very sensitive to initial conditions as well as to small variations in model parameters. Changing parameters as tertiary as the viscous damping of the pistons can change the model's prediction from a foot-first landing to head-first landing. The model is compared to time histories of angular velocity for two different animations in Fig. 4. We believe that the model captures the general behavior of the system well enough that it is a useful tool for understanding the capabilities and limitations of the system. In practice, the model is used to inform a first guess at the timing required for a desired stunt, and then the timing is iteratively refined based on actual results. In the future, creating a simplified but still-informative model of swinging

dynamics is a goal of this project.

B. Mid-air Dynamics

Once in-flight, the physics of motion are relatively simple. If the principal moment of inertia is closely aligned with the angular momentum vector, then we can write:

$$L = I\omega \tag{1}$$

where I is the principal moment of inertia around the axis of rotation and ω is the angular velocity.

If the moment of inertia changes from I_1 to I_2, the change in angular velocity is given by:

$$\omega_{new} = \frac{I_1}{I_2}\omega_{old}. \tag{2}$$

This is simplest if the change in inertia from one state to another is smooth, fast, and monotonic, and if the angular velocity is in good alignment with the desired axis of rotation. In practice we found that tucking a little before release helped slow or eliminate twist. The pneumatic cylinders used provide a fast transition, but are under-damped and create a strong ringing effect which makes accurate measurement and simulation of this stage more difficult. If we disregard this ringing effect, the results of un-tucking can be characterized by an average angular velocity before, during, and after the un-tuck event, very similar to the analysis performed in [26]. This analysis should be modified due to the fact that the un-tuck event changes the relative angles of each body segment, so a constant angular displacement, θ_{offset}, can be added to the result.

Using the onboard accelerometer, the onboard laser range-finder, and a model of expected dynamics, we can estimate the amount of time left in the air, T_a, based on our estimate of height and vertical velocity at a given time t_0:

$$T_a = \frac{v_0}{g} + \sqrt{\left(\frac{v_0}{g}\right)^2 + \frac{2h_0}{g}} \tag{3}$$

where h_0 is the estimated height at time t_0, v_0 is the estimated vertical component of velocity at time t_0, and g is acceleration due to gravity.

We can use the following formula to estimate the final orientation, θ_{final}, if the release were to be commanded immediately:

$$\theta_{\text{final}} = \theta + \theta_{\text{offset}} + \omega R_t T_t + \omega R_f \left(T_a - (t - t_0) - T_t\right) \tag{4}$$

where θ is the current estimated angle between the center link and the ground, θ_{offset} is the expected displacement due to re-configuration of limbs, ω is the current angular velocity, R_t is the predicted ratio between the current angular velocity and the average angular velocity during the transition, T_t is the predicted time for the transition, R_f is the predicted ratio between the current and final angular velocities, t is the current time, and t_0 is the time at which T_a was last estimated. R_f is found empirically by observing the differnce in angular velocity between tucked and untucked configurations mid-flight. R_t is determined by comparing the average angular velocity during the untucking motion to the angular velocity in the tucked position.

C. Predicted capabilities

Launching capability, in terms of the number of possible somersaults and the range of possible landing locations, is constrained by the total available energy of the system. For Stickman, the energy stored in the air tanks is about an order of magnitude less than the energy stored in potential energy at the beginning of the swing. The main determinant of capability, then, is the way that energy can be allocated between linear and angular momentum in each axis. For the majority of the following analysis, we will assume that tucking occurs only after we have released from the pendulum.

In Stickman's pendulum-based launch, the relationship between linear and angular momentum is constrained by rigid body kinematics. Only those velocities which maintain the absolute lengths of the two pendulum links are allowed. Numerically simulating the full range of kinematically possible velocity configurations gives us an upper bound on what combinations of angular and linear velocities are possible given our experimental setup. We can then use these velocities to calculate the final position and total rotation of the robot, as shown in Fig. 5.

This broad range of possible outcomes is slightly misleading as it includes situations which are kinematically possible but practically infeasible. To get a more reasonable estimate of total capability, we can limit the angular velocity of the second link to prevent it from exceeding 180 degrees in amplitude under typical loading conditions.

We can then take our previous kinematic analysis and discard any results which result in an angular velocity greater than this value, which produces the top right graph in Fig. 5.

This theoretical limit then becomes a way of measuring the capability of a proposed control scheme while on the pendulum. If the area of possible states covered by a proposed method covers a significant percentage of the theoretical limits, then we can be confident that we are not artificially limiting robotic capability by our approach.

Two possible control methods can now be explored and compared using the full dynamic model of Stickman. The first method is to simply change the initial angle between the center link of the robot and the world-frame horizontal while satisfying the constraint that no part of Stickman is allowed to penetrate the ceiling. The results of this method over varying release times are illustrated in the bottom left corner of Fig. 5.

The second method is to begin the tuck while still on the pendulum. This changes the length and inertia of Stickman, thus changing the frequency of the second-order pendulum behavior and changing the relative phase of angular and

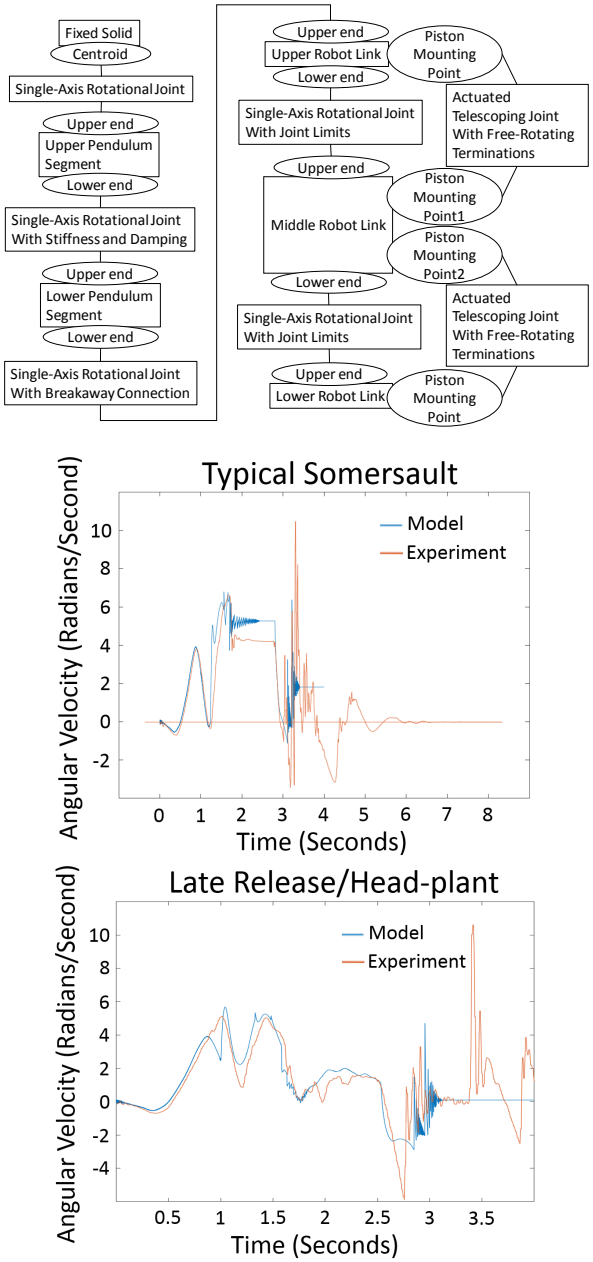

Fig. 4: Top: schematic view of physical elements modeled in Simscape Multibody, consisting of joints and rigid body elements. Middle: model versus experiment for a typical somersault animation. Bottom: model versus experiment for an early tuck, late release headplant. In the lower figures, blue represents simulated angular velocity and red represents actual angular velocity as measured by the onboard gyroscope.

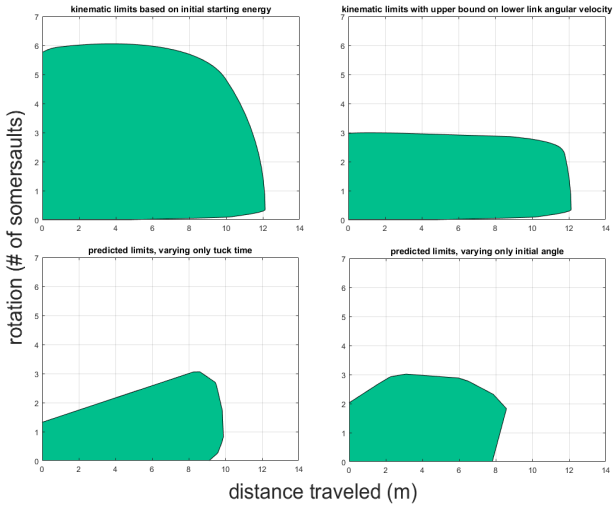

Fig. 5: Reachable states with various constraints - kinematic and energetic possibility (top left), kinematic possibility given a maximum second link amplitude (top right), full simulation sweep over different tuck times (bottom left), full simulation sweep over different initial angles (bottom right).

linear momentum. The results of this method are shown in the bottom right of Fig. 5.

Once in the air, the robot has a fixed amount of angular momentum available and a fixed amount of time before the ballistic trajectory impacts the ground.

The mid-air capability of the robot can be measured by how much it is able to change its final angle given an initial angular momentum. In the case of stickman, the ratio between tucked and untucked moments of inertia is about 1 to 3, which means that for a flight which can produce two thirds of a somersault in the untucked position, the robot can achieve an actual number of rotations between that two thirds of a rotation and two full rotations.

VI. Results

Stickman achieved total flight distances ranging from 5 to 11 meters. No serious effort was made to control final position run to run, but a typical animation showed a standard deviation in landing position of about 20 centimeters for five trials.

Based on a combination of modeling and iterative refinement, Stickman achieved three distinct rotation profiles for Stickman – zero, one, and two backflips. Image sequences of these three different animations are shown in Fig. 6.

Simulations also predicted the ability to perform half of a forward flip if a large enough initial angle was used. Tests pursuing this goal achieved the angular velocity necessary while still on the pendulum, but excessive loading on the latch caused a jamming effect that prevented the robot from releasing at the correct time.

A simple control law was used to attempt to ensure Stickman landed in gross alignment with the mat. Using a naive estimate of the difference between distance measurements

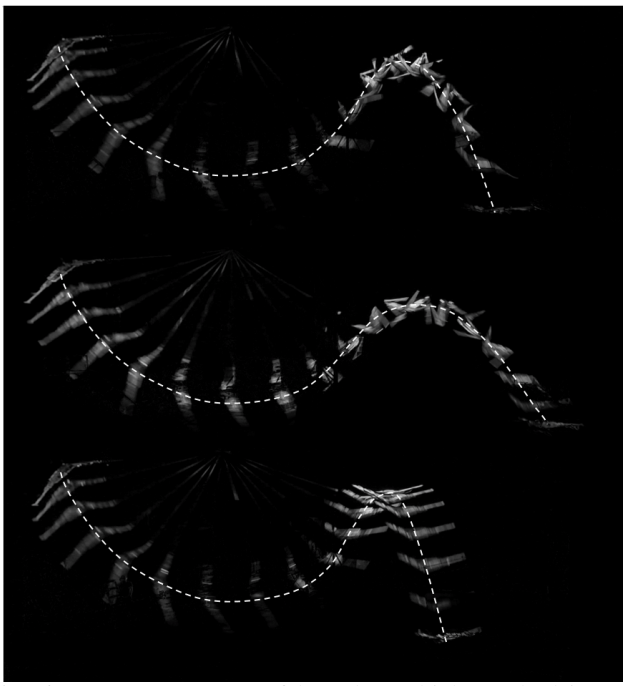

Fig. 6: Image sequences of launches which resulted in two (top), one (middle), and zero (bottom) total backflips.

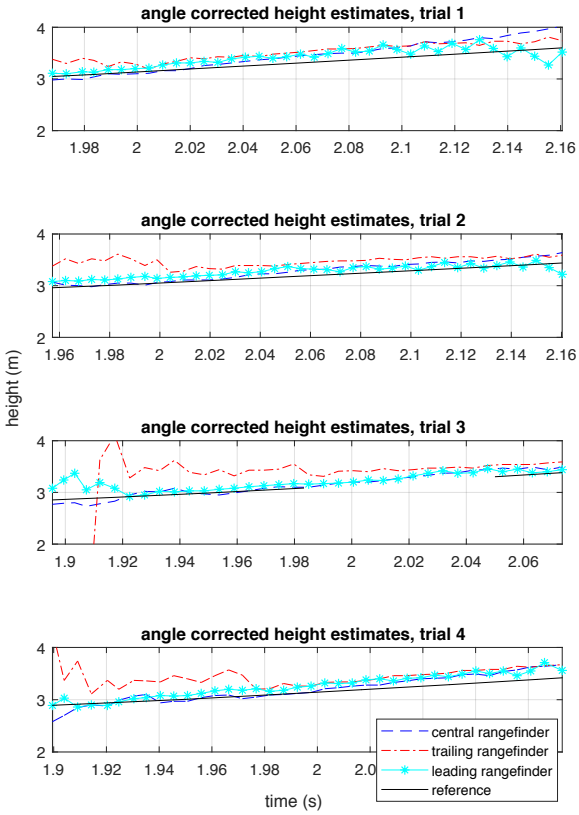

Fig. 7: Comparison of height estimates using angle corrected laser rangefinder readings.

over the last ten trials, the robot attempted to calculate time left in the air and adapt to its measured angular velocity and estimated flight time.

The robot uses the angle estimate from the IMU to correct for the angle at which the laser rangefinders collect a particular reading. Resulting height estimates are compared to the ground truth from the motion capture system in Fig. 7.

The robot landed with an average angular error of 27 degrees of over-rotation, with a standard deviation of 28 degrees. A range of typical landings is shown in Fig.

Position and velocity can also be estimated by using the IMU to estimate vertical acceleration. This was found to work well on the pendulum, but encountered a discontinuity around the time of release, as illustrated in Fig. 9.

In future work, we will investigate fusing the information from the imu and the laser rangefinder to achieve a better estimate of height and velocity, allowing us to improve the accuracy of final angle control.

VII. Conclusion and Future Work

Stickman emulates the behavior of human performers using a very limited set of sensing and actuation capabilities. It is able to successfully perform several different somersaulting stunts by changing initial orientation and the timing of tuck, release, and untuck. The onboard sensors are able to track the angle, height, and velocity of the robot.

In future work, we will pursue more advanced sensing and control strategies to increase the repeatability of the robot. Initial tests are already underway.

As the robot progresses towards more interesting stunts, it will likely require more degrees of freedom to allow control in other axes of rotation, and possibly position as well.

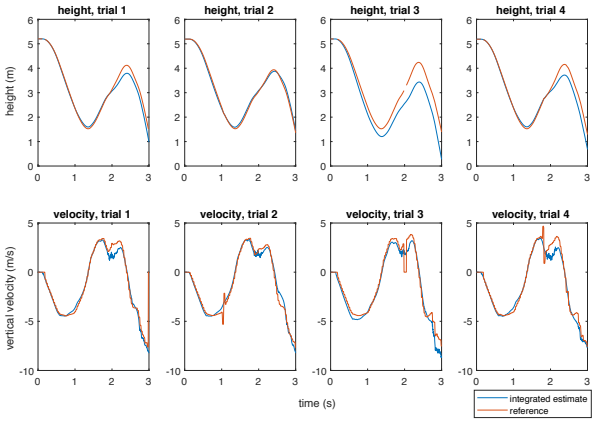

Fig. 8: Comparison of height and velocity estimation using integrated vertical acceleration. Note the discrepancy beginning around the time of release (t=1.6) for runs 1, 2, and 4.

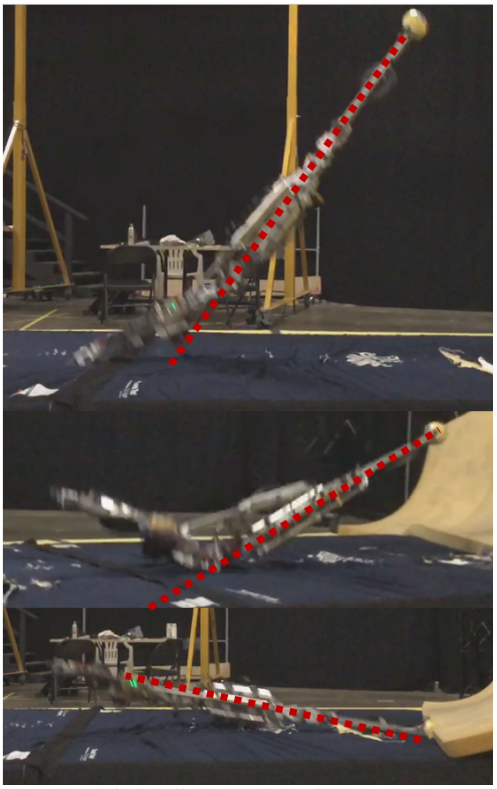

Fig. 9: Range of landing angles for typical experiments using combination of IMU and laser rangefinder position estimation, showing an over-rotation (top), an average landing (middle) and an under-rotation (bottom).

This effort will be facilitated by ongoing efforts in refining the simulation of the robot and attempting to develop simplified models that provide more intuition for the behavior of the system. Some early models based on observing the robot's angular momentum instead of its angular velocity appear initially promising.

VIII. Acknowledgments

The authors would like to thank Tony Dohi, Mark Setrakian, and Shannon Shea for providing crucial logistical support for this project.

References

[1] M. R. Yeadon, "The biomechanics of twisting somersaults part i: Rigid body motions," *Journal of Sports Sciences*, vol. 11, no. 3, pp. 187–198, 1993.

[2] R. Armour, K. Paskins, A. Bowyer, J. Vincent, and W. Megill, "Jumping robots: a biomimetic solution to locomotion across rough terrain," *Bioinspiration & biomimetics*, vol. 2, no. 3, p. S65, 2007.

[3] M. Noh, S. W. Kim, S. An, J. S. Koh, and K. J. Cho, "Flea-inspired catapult mechanism for miniature jumping robots," *IEEE Transactions on Robotics*, vol. 28, no. 5, pp. 1007–1018, Oct 2012.

[4] M. Kovac, M. Fuchs, A. Guignard, J. C. Zufferey, and D. Floreano, "A miniature 7g jumping robot," in *2008 IEEE International Conference on Robotics and Automation*, May 2008, pp. 373–378.

[5] J. Zhao, J. Xu, B. Gao, N. Xi, F. J. Cintrón, M. W. Mutka, and L. Xiao, "Msu jumper: A single-motor-actuated miniature steerable jumping robot," *IEEE Transactions on Robotics*, vol. 29, no. 3, pp. 602–614, June 2013.

[6] M. H. Raibert, *Legged robots that balance*. MIT press, 1986.

[7] D. W. Haldane, M. Plecnik, J. Yim, and R. Fearing, "Robotic vertical jumping agility via series-elastic power modulation," *Science Robotics*, vol. 1, no. 1, p. eaag2048, 2016.

[8] A. Degani, S. Feng, H. B. Brown, K. M. Lynch, H. Choset, and M. T. Mason, "The parkourbot-a dynamic bowleg climbing robot," in *Robotics and Automation (ICRA), 2011 IEEE International Conference on*. IEEE, 2011, pp. 795–801.

[9] M. Kovač, O. Fauria, J.-C. Zufferey, D. Floreano, *et al.*, "The epfl jumpglider: A hybrid jumping and gliding robot with rigid or folding wings," in *Robotics and Biomimetics (ROBIO), 2011 IEEE international conference on*. IEEE, 2011, pp. 1503–1508.

[10] A. L. Desbiens, M. T. Pope, D. L. Christensen, E. W. Hawkes, and M. R. Cutkosky, "Design principles for efficient, repeated jumpgliding," *Bioinspiration & biomimetics*, vol. 9, no. 2, p. 025009, 2014.

[11] E. Beyer and M. Costello, "Measured and simulated motion of a hopping rotochute," *Journal of guidance, control, and dynamics*, vol. 32, no. 5, pp. 1560–1569, 2009.

[12] T. Libby, T. Y. Moore, E. Chang-Siu, D. Li, D. J. Cohen, A. Jusufi, and R. J. Full, "Tail-assisted pitch control in lizards, robots and dinosaurs," *Nature*, vol. 481, no. 7380, pp. 181–184, 2012.

[13] C. Casarez, I. Penskiy, and S. Bergbreiter, "Using an inertial tail for rapid turns on a miniature legged robot," in *Robotics and Automation (ICRA), 2013 IEEE International Conference on*. IEEE, 2013, pp. 5469–5474.

[14] A. M. Johnson, T. Libby, E. Chang-Siu, M. Tomizuka, R. J. Full, and D. E. Koditschek, "Tail assisted dynamic self righting," in *Proceedings of the Fifteenth International Conference on Climbing and Walking Robots*, July 2012, pp. 611–620.

[15] Z. Weng and H. Nishimura, "Final-state control of a two-link cat robot by feedforward torque inputs," in *Advanced Motion Control, 2000. Proceedings. 6th International Workshop on*. IEEE, 2000, pp. 264–269.

[16] K. YAMAFUJI, T. KOBAYASHI, and T. KAWAMURA, "Elucidation of twisting motion of a falling cat and its realization by a robot," *Journal of the Robotics Society of Japan*, vol. 10, no. 5, pp. 648–654, 1992.

[17] T. Kawamura, K. Yamafuji, and T. Kobayashi, "Study on posture control and soft landing of a free falling robot.(1st report, posture control by turning motion of a cat)," *Transactions of the Japan Society of Mechanical Engineers*, vol. 57, no. 544, pp. 3895–3900, 1991.

[18] S.-k. Yun, A. Goswami, and Y. Sakagami, "Safe fall: Humanoid robot fall direction change through intelligent stepping and inertia shaping," in *Robotics and Automation, 2009. ICRA'09. IEEE International Conference on*. IEEE, 2009, pp. 781–787.

[19] S.-H. Hyon, N. Yokoyama, and T. Emura, "Back handspring of a multi-link gymnastic robot—reference model approach," *Advanced Robotics*, vol. 20, no. 1, pp. 93–113, 2006.

[20] B. Ugurlu and A. Kawamura, "On the backward hopping problem of legged robots," *IEEE Transactions on Industrial Electronics*, vol. 61, no. 3, pp. 1632–1634, 2014.

[21] S. Ha, Y. Ye, and C. K. Liu, "Falling and landing motion control for character animation," *ACM Transactions on Graphics (TOG)*, vol. 31, no. 6, p. 155, 2012.

[22] J. T. Bingham, J. Lee, R. N. Haksar, J. Ueda, and C. K. Liu, "Orienting in mid-air through configuration changes to achieve a rolling landing for reducing impact after a fall," in *Intelligent Robots and Systems (IROS 2014), 2014 IEEE/RSJ International Conference on*. IEEE, 2014, pp. 3610–3617.

[23] R. R. Playter and M. H. Raibert, "Control of a biped somersault in 3d," in *Intelligent Robots and Systems, 1992., Proceedings of the 1992 lEEE/RSJ International Conference on*, vol. 1. IEEE, 1992, pp. 582–589.

[24] S. Kuindersma, R. Deits, M. Fallon, A. Valenzuela, H. Dai, F. Permenter, T. Koolen, P. Marion, and R. Tedrake, "Optimization-based locomotion planning, estimation, and control design for the atlas humanoid robot," *Autonomous Robots*, vol. 40, no. 3, pp. 429–455, 2016.

[25] J. Nakanishi, T. Fukuda, and D. E. Koditschek, "A brachiating robot controller," *IEEE Transactions on Robotics and Automation*, vol. 16, no. 2, pp. 109–123, 2000.

[26] M. Pope and G. Niemeyer, "Falling with style: Sticking the landing by controlling spin during ballistic flight," in *Intelligent Robots and Systems (IROS 2017), 2017 IEEE/RSJ International Conference on*. IEEE, 2017.